

Environmental Science and Pollution Research

Confocal microscopy 3D imaging of diesel particulate matter

--Manuscript Draft--

Manuscript Number:	ESPR-D-20-09129R1	
Full Title:	Confocal microscopy 3D imaging of diesel particulate matter	
Article Type:	Short Research and Discussion Article	
Corresponding Author:	David Wertheim Kingston University Kingston, Surrey UNITED KINGDOM	
Corresponding Author Secondary Information:		
Corresponding Author's Institution:	Kingston University	
Corresponding Author's Secondary Institution:		
First Author:	Lisa Miyashita	
First Author Secondary Information:		
Order of Authors:	Lisa Miyashita	
	Gary Foley	
	Ian Gill	
	Gavin Gillmore	
	Jonathan Grigg	
	David Wertheim	
Order of Authors Secondary Information:		
Funding Information:	Barts Charity, UK (MGU0312)	Professor Jonathan Grigg
	The Medical College of Saint Bartholomew's Hospital Trust (17/LO/1752)	Professor Jonathan Grigg
Abstract:	<p>To date diesel particulate matter (DPM) has been described as aggregates of spherule particles with a smooth appearing surface. We have used a new colour confocal microscope imaging method to study the 3D shape of diesel particulate matter (DPM); we observed that the particles can have sharp jagged appearing edges and consistent with these findings, 2D light microscopy demonstrated that DPM adheres to human lung epithelial cells. Importantly, the slide preparation and confocal microscopy method applied avoids possible alteration to the particles' surfaces and enables colour 3D visualisation of the particles. From twenty-one PM10 particles, the mean (standard deviation) major axis length was 5.6 (2.25) μm with corresponding values for the minor axis length of 3.8 (1.25) μm. These new findings may help explain why air pollution particulate matter (PM) has the ability to infiltrate human airway cells, potentially leading to respiratory tract, cardiovascular and neurological disease.</p>	

[Click here to view linked References](#)

1 **Confocal microscopy 3D imaging of diesel particulate matter**

2

3

4 Lisa Miyashita^{1*} and Gary Foley^{1*}, Ian Gill², Gavin Gillmore³, Jonathan Grigg¹, David

5 Wertheim².

6 * These authors have contributed equally to the manuscript and wish to have joint

7 first authorship if accepted for publication.

8 1. Centre for Genomics and Child Health, Blizard Institute, Queen Mary University of

9 London, UK

10 2. Faculty of Science, Engineering and Computing, Kingston University, Surrey, UK

11 3. Faculty of Science, Engineering and Computing, Kingston University, Surrey, UK

12 (current address: School of Science, Bath Spa University, Bath, UK.)

13

14 **Address for correspondence:** David Wertheim, Faculty of Science, Engineering and

15 Computing, Kingston University, Surrey. KT1 2EE. UK. E-mail: D.Wertheim@kingston.ac.uk

16 Tel: +44 (0)20 8417 2662

17

18 **Keywords:** particulate matter; [diesel particulate matter](#); confocal microscopy; 3D

19 microscope imaging.

20

21

22

23 **Abstract**

24 To date [diesel particulate matter \(DPM\)](#) has been described as aggregates of spherule
25 particles with a smooth appearing surface. We have used a new colour confocal microscope
26 imaging method to study the 3D shape of [diesel particulate matter \(DPM\)](#); we observed that
27 the particles can have sharp jagged appearing edges and consistent with these findings, 2D
28 light microscopy demonstrated that DPM adheres to human lung epithelial cells.
29 Importantly, the slide preparation and confocal microscopy method applied avoids possible
30 alteration to the particles' surfaces and enables colour 3D visualisation of the particles.
31 From twenty-one PM₁₀ particles, the mean (standard deviation) major axis length was
32 5.6 (2.25) μm with corresponding values for the minor axis length of 3.8 (1.25) μm . These
33 new findings may help explain why air pollution particulate matter (PM) has the ability to
34 infiltrate human airway cells, potentially leading to respiratory tract, cardiovascular and
35 neurological disease.
36

37 **Introduction:**

38 It has been suggested that air pollution is a major cause of premature death and is a
39 recognised risk factor leading to human respiratory disease (Anderson et al. 2012, WHO
40 2018, Khomenko et al. 2021). A major component of air pollution is in the form of
41 particulate matter (PM). The impact of air pollution PM on human health is not restricted to
42 effects in the lungs, with several studies identifying a link with heart disease, neurological
43 disease and adverse pregnancy outcomes (Anderson et al. 2012, Klepac et al. 2018, Ren et
44 al. 2019, Wu et al. 2019). Air pollution derived PM has a number of natural causes such as
45 wildfires and volcanic eruptions but in urban areas anthropogenic sources such as emissions
46 from traffic predominate (Grigg 2012). In particular, emissions from diesel engines are
47 considered to be one of the largest contributors to environmental pollution (Lloyd and
48 Cackette 2001). Overall, PM released from combustible sources is primarily composed of
49 black carbon (Anderson et al. 2012) and is grouped into three main categories based on
50 aerodynamic diameter: PM_{10} ($< 10 \mu m$), $PM_{2.5}$ ($< 2.5 \mu m$) and ultrafine PM ($< 1 \mu m$). The size
51 determines its aerodynamic characteristics and consequently its capacity to penetrate the
52 alveolar wall and enter the bloodstream (Brugha et al. 2014). Evidence of combustion
53 derived PM has recently been reported in both brain and heart tissue (Maher et al. 2016,
54 Calderon-Garciduenas et al. 2019).

55

56 Numerous studies have focused on the immunological effect of air pollution derived PM,
57 however, research defining the morphology of this PM is lacking. It was demonstrated that
58 non-pollution derived particles with a more defined, sharper edge displaced lung surfactant
59 to a larger degree than those with a spherical composition, allowing these particles to be
60 more readily internalised by the lung epithelium (Gerber et al. 2006). To date, combustion-

61 derived PM is reported to consist of aggregates of carbonaceous spherules with a smooth
62 appearing surface (Yang et al. 2016, Zeb et al. 2018). Recently, a novel method was
63 developed to visually assess volcanic PM in 3D by high resolution laser scanning confocal
64 microscopy (Wertheim et al. 2017). In contrast to the previously suggested spherical nature
65 of diesel PM, the morphology of some volcanic particulates were shown to be jagged.

66

67 To help understand the morphology of diesel particulate matter DPM also known as diesel
68 exhaust particulate (DEP) and mode of action on lung epithelial cell invasion, our study
69 aimed to investigate the 3D structure of DPM, and its interaction with human lung
70 epithelial cells.

71

72 **Materials and Methods:**

73 DPM was acquired in powder form from the National Institute of Standards and Technology
74 (NIST,SRM2975,USA). Double-sided adhesive carbon disks (12mm, Agar Scientific Ltd., UK)
75 were adhered to microscope slides (VWR International, UK). DPM was sieved through a
76 mesh filter (50µm, VWR) onto the carbon disk slides to prevent aggregation of particles.
77 DPM slides were then imaged using a LEXT OLS4100 confocal microscope (Olympus
78 Corporation, Japan) with a 405nm laser. Images with resolution 1024 x 1024 pixels were
79 taken using a x100 objective lens (numerical aperture 0.95) and collected using the fine
80 mode setting. Imaging threshold parameters were set by adjusting the upper limit to just
81 above the top of the particles and the lower limit to just below the level of the adhesive disk
82 (Wertheim et al. 2017). Particle size was measured using the Olympus OLS4100 microscope
83 system software (Olympus Corporation, Japan). For size measurements, particles were
84 considered as approximately elliptical and the longest 2D axis was termed 'major axis' and

85 the perpendicular axis termed 'minor axis'; the maximum 3D height was determined using a
86 profile tool in the software. Descriptive statistics of particle size data were calculated using
87 Minitab v19 (Minitab Inc., USA).

88

89 A549 adenocarcinomic human alveolar epithelial cells were seeded into Nunc® chamber
90 well slides (Merck, UK) overnight and incubated with 10µg/ml DPM for 2 hours, thoroughly
91 washed and stained (Hemacolor®, VWR international). Fifty images with resolution 746 x
92 500 pixels, were taken at random by light microscopy (Nikon Eclipse 80i) using a x100
93 objective lens.

94

95 **Results:**

96 Images were successfully acquired with the confocal microscope in 2D and 3D from the
97 slides and demonstrated a variety of DPM shapes and sizes. A stitched image consisting of 9
98 adjacent partially overlapping images in figure 1 demonstrates the heterogeneous nature of
99 particle morphology over a larger area. The \leq PM₁₀ particles frequently had sharp, jagged
100 appearing edges; the images show comparison with larger particulate aggregates (figure 2A
101 and 2B) and an individual particle (figure 2C). Some particles imaged may in part consist of
102 agglomeration of fine particles. The images revealed particles of a comparable nature in
103 colour and shape, making the likelihood of contamination low. As the microscope
104 illumination and imaging are from above the sample and the DPM is opaque, the shape of
105 the bottom surface on the adhesive carbon disk could not be discerned in detail.

106

107 From measurements of twenty-one \leq PM₁₀ particles, the mean (standard deviation) major
108 axis length was 5.6 (2.25)µm with corresponding values for the minor axis length 3.8

109 (1.25) μm and the ratio major / minor was 1.5 (0.46) μm ; the ratio also suggests particles 2D
110 cross-section are often not circular. Culture of A549 lung epithelial cells with 10 $\mu\text{g}/\text{ml}$ DPM
111 *in vitro*, followed by vigorous washing to remove unbound particles, demonstrated that
112 DPM can exhibit adherence to the cells (Figure 3).

113

114

115 **Discussion:**

116 Epidemiological studies have demonstrated a likely link between PM concentration
117 [exposure](#) and the onset of respiratory, cardiovascular and neurological disease (Anderson et
118 al. 2012). For example, [exposure to](#) elevated PM concentration is suggested to be related to
119 the incidence of hospital admission (Wei et al. 2019, de Aguiar Pontes Pamplona et al. 2020)
120 and adverse health effects in conditions such as respiratory disease for instance asthma
121 (Grigg 2012, Thurston et al. 2020), heart disease (Tian et al. 2019, de Aguiar Pontes
122 Pamplona et al. 2020, Chen et al. 2020) and stroke (Huang et al. 2019); recently it has also
123 been suggested that [exposure to](#) high levels of particulate matter may be associated with
124 increased blood pressure in adults (Xu et al. 2020). An increased incidence of health related
125 disease, likely associated with high levels of ambient PM, can also occur following volcanic
126 eruptions (Forbes et al. 2003, Oudin et al. 2013, Carlsen et al. 2015) and forest fires
127 (Dennekamp and Abramson 2011).

128

129 The underlying mechanisms that drive elevated levels of ambient PM to increase disease
130 onset or exacerbation remains unclear. If this were better understood it could help in the
131 development of novel strategies to ameliorate the adverse effects of elevated PM that
132 result from human activity and natural events. For example, studies have demonstrated the
133 ability of PM to be internalised by, or tightly adhere to airway epithelial cells (Colasanti et al.
134 2018), as well as lung tissue (Mäkelä et al. 2019), however the mode of action is yet to be
135 fully elucidated. Furthermore, PM from various sources are likely to invoke differences in
136 disease severity. This is demonstrated in a study that identified Baltimore PM to induce a
137 much greater inflammatory response compared to that in New York City (Gour et al. 2018).

138 Defining the inflammatory profile of PM [constituents](#) may therefore be an important factor
139 in predicting adverse health effects.

140

141 Several methods of imaging aerosol particles, other than confocal microscopy, have been
142 listed by Li et al. 2016. Indeed previous studies of the appearance of particulate matter have
143 generally used 2D imaging such as investigations based on optical microscopy (Davis and
144 Jixiang 2000, Tian et al. 2017, Koval et al. 2018), Scanning Electron Microscopy (SEM) ([Yang
145 et al. 2016](#), Selley et al. 2020), Transmission Electron Microscopy (TEM) (Bérubé et al. 1999,
146 Chandler et al. 2007, Liati et al. 2012) or for 3D imaging [of particles, stereo SEM \(Mills and
147 Rose 2010\)](#). Previous studies of diesel exhaust particulate morphology have often used SEM
148 or TEM (Figler et al. 1996, Liati et al. 2012, Liati et al. 2013, Baldelli et al. 2020). Stereo SEM
149 can generate 3D reconstruction of particles with such techniques being reliant on
150 homologous points and interpolation (Prousevitch et al. 2011); furthermore as electrons
151 are used to image the sample in SEM and TEM, there is no simultaneous overlaid true colour
152 image. However, our laser scanning confocal microscopy technique allows direct 3D
153 measurement of particles together with true colour visualisation.

154

155 In contrast to a previous study that depicted haze related urban PM as spherical based on
156 2D SEM (Zeb et al. 2018), we have shown using 3D confocal imaging that [DPM](#) can contain
157 particles with sharp appearing edges. [Diesel emission particles can vary in size from fine
158 particles less than 100nm to several micrometers \(Liati et al. 2013, Rocha and Corrêa 2018\);
159 in view of the range of DPM size it is possible that at least some particles imaged with
160 confocal microscopy may consist of fine particle agglomeration.](#) A recent study has reported
161 that brake dust particles can also have jagged edges (Selley et al. 2020). DPM matter is

162 created by controlled spontaneous combustion at high temperatures within the engine
163 chamber, leading to the formation of fragments with varying morphology, some of which
164 have sharp appearing edges. These jagged edges may help to explain the observed
165 adherence of [DPM](#) to lung epithelial cells (Figure 3) in our study.

166

167 More research is needed to identify the direct effect morphology has on cell integrity, and
168 the observed adherence of [DPM](#) to alveolar epithelial cells cannot be explained by
169 morphology alone. However, as sharp non-pollution derived particles are more readily
170 internalised by lung epithelium compared to those more spherical (Gerber et al. 2006), it is
171 plausible that the observed jagged morphology of [DPM](#) has similar effects in the airways.
172 Furthermore, sharp edged particles are reported to significantly enhance cytokine release
173 compared to smooth, spherule particles of the same size, suggesting that morphology has
174 an important role in the inflammatory potential of PM (Lebre et al. 2017). [In addition it has
175 been suggested that adverse health effects are associated with the interaction of PM_{2.5}
176 surface groups with biomolecules in lung fluid \(Zhou et al. 2016\).](#)

177

178 We postulate that these sharp edges more readily present the airway immune system with
179 foreign epitopes; initiating cellular uptake by alveolar macrophages (AM) which have been
180 shown to phagocytose air pollution derived PM in a similar manner to bacteria (Brugha et al.
181 2014). Furthermore, jagged edges combined with a small surface area may impact on cell
182 integrity at the molecular level by either anchoring to the cell membrane and/or initiating
183 van der Waals forces, both of which could induce cellular internalisation. These forces have
184 previously been shown to have important biological functions and may represent a novel
185 mechanism for cellular infiltration (Autumn et al. 2000).

186

187 Importantly, the methodology adopted in this study allows collection of colour 3D images of
188 particles without the need for coating or mounting in a substrate thus avoiding possible
189 alteration or damage to the surface of the particles. Fine particles, which are particularly
190 detrimental to human health, previously observed with 2D microscopy can now be clearly
191 visualised and defined in colour and in 3D.

192

193

194

195 **Conclusion:**

196 This study has used a novel method to show that microscopic **DPM** matter, which have been
197 previously characterised as of spherical shape, includes particles with sharp appearing
198 edges; this jagged appearance may aid the ability of particles to tightly adhere to epithelial
199 cells and increase airway inflammation. We suggest that the observed particle morphology
200 may enhance the capacity for air pollution derived PM to enter the human body and
201 subsequently cause adverse health effects. This straightforward novel methodology
202 provides a means to compare air pollution derived particulate morphology from various
203 sources, to help define their inflammatory potential, determine the consequent effect on
204 cell integrity and importantly, contribute to the development of ameliorating measures.

205

206

207

208 **References**

209 Anderson JO, Thundiyil JG, Stolbach A. Clearing the air: a review of the effects of particulate
210 matter air pollution on human health. *J Med Toxicol.* 2012;8(2):166-75.

211

212 Autumn K, Liang YA, Hsieh ST, Zesch W, Chan WP, Kenny TW, et al. Adhesive force of a
213 single gecko foot-hair. *Nature.* 2000;405(6787):681-5.

214

215 Baldelli A, Trivanovic U, Corbin JC, Lobo P, Gagné S, Miller JW, Kirchen P and Rogak S.
216 Typical and Atypical Morphology of Non-volatile Particles from a Diesel and Natural Gas
217 Marine Engine. *Aerosol and Air Quality Research.* 2020; 20: 730-740.

218 doi.org/10.4209/aaqr.2020.01.0006

219

220 Bérubé KA, Jones TP, Williamson BJ, Winters C, Morgan AJ and Richards RJ. Physicochemical
221 characterisation of diesel exhaust particles: Factors for assessing biological activity.

222 *Atmospheric Environment.* 1999; 33:1599-1614.

223

224 Brugha RE, Mushtaq N, Round T, Gadhvi DH, Dundas I, Gaillard E, et al. Carbon in airway
225 macrophages from children with asthma. *Thorax.* 2014;69(7):654-9.

226

227 Calderon-Garciduenas L, Gonzalez-Maciel A, Mukherjee PS, Reynoso-Robles R, Perez-Guille
228 B, Gayosso-Chavez C, et al. Combustion- and friction-derived magnetic air pollution
229 nanoparticles in human hearts. *Environ Res.* 2019;176:108567.

230

231 Carlsen HG, Gislason T, Forsberg B, Meister K, Thorsteinsson T, Jóhannsson T,
232 Finnbjornsdottir R, Oudin A. Emergency Hospital Visits in Association With Volcanic Ash,
233 Dust Storms and Other Sources of Ambient Particles: A Time-Series Study in Reykjavík,
234 Iceland. *Int J Environ Res Public Health*. 2015;12:4047-59. doi: 10.3390/ijerph120404047.
235
236 [Chandler MF, Teng Y and Koylu UO. Diesel engine particulate emissions: A comparison of](#)
237 [mobility and microscopy size measurements. *Proceedings of the Combustion Institute*.](#)
238 [2007; 31: 2971-2979.](#)
239
240 Chen C, Liu X, Wang X, Qu W, Li W, Dong L. Effect of air pollution on hospitalization for acute
241 exacerbation of chronic obstructive pulmonary disease, stroke, and myocardial infarction.
242 *Environ Sci Pollut Res Int*. 2020;27(3):3384-3400. doi:10.1007/s11356-019-07236-x
243
244 Colasanti T, Fiorito S, Alessandri C, Serafino A, Andreola F, Barbati C, et al. Diesel exhaust
245 particles induce autophagy and citrullination in Normal Human Bronchial Epithelial cells. *Cell*
246 *Death Dis*. 2018;9(11):1073.
247
248 Davis BL and Jixiang G. Airborne particulate study in five cities of China. *Atmospheric*
249 *Environment* 2000; 34: 2703-2711.
250
251 de Aguiar Pontes Pamplona Y, Arbex MA, Braga ALF, Pereira LAA, Martins LC. Relationship
252 between air pollution and hospitalizations for congestive heart failure in elderly people in
253 the city of São Paulo. *Environ Sci Pollut Res Int*. 2020; 27: 18208-18220.
254 doi:10.1007/s11356-020-08216-2.

255

256 Dennekamp M and Abramson MJ. The Effects of Bushfire Smoke on Respiratory Health.
257 *Respirology* 2011; 16: 198-209. doi: 10.1111/j.1440-1843.2010.01868.x.

258

259 Figler B, Sahle W, Krantz S and Ulfvarson U. Diesel exhaust quantification by scanning
260 electron microscope with special emphasis on particulate size distribution. *Science of The*
261 *Total Environment*. 1996; 193: 77-83. doi.org/10.1016/S0048-9697(96)05328-4.

262

263 [Forbes L, Jarvis D, Potts J, Baxter PJ. Volcanic ash and respiratory symptoms in](#)
264 [children on the island of Montserrat, British West Indies. *Occup. Environ. Med.* 2003; 60:](#)
265 [207–211.](#)

266

267 Gerber PJ, Lehmann C, Gehr P, Schurch S. Wetting and spreading of a surfactant film on
268 solid particles: influence of sharp edges and surface irregularities. *Langmuir*.
269 2006;22(12):5273-81.

270

271 Gour N, Sudini K, Khalil SM, Rule AM, Lees P, Gabrielson E, Groopman JD, Lajoie S and Singh
272 A. . Unique pulmonary immunotoxicological effects of urban PM are not recapitulated solely
273 by carbon black, diesel exhaust or coal fly ash. *Environ Res.* 2018; 161:304-313.

274

275 Grigg J. Traffic-derived air pollution and lung function growth. *Am J Respir Crit Care Med*.
276 2012;186(12):1208-9.

277

278 Huang K, Liang F, Yang X, Liu F et al. Long Term Exposure to Ambient Fine Particulate Matter
279 and Incidence of Stroke: Prospective Cohort Study From the China-PAR Project. *BMJ* 2019
280 Dec 30;367:l6720. doi: 10.1136/bmj.l6720.

281

282 [Khomenko S, Cirach M, Pereira-Barboza E, Mueller N, Barrera-Gómez J, Rojas-Rueda D, de](#)
283 [Hoogh K, Hoek G, Nieuwenhuijsen M. Premature mortality due to air pollution in European](#)
284 [cities: a health impact assessment. *Lancet Planet Health*. 2021 Jan 19:S2542-5196\(20\)30272-](#)
285 [2. doi: 10.1016/S2542-5196\(20\)30272-2.](#)

286

287 Klepac P, Locatelli I, Korošec S, Künzli N and Kukec A. Ambient air pollution and pregnancy
288 outcomes: A comprehensive review and identification of environmental public health
289 challenges. *Environ Res*. 2018; 167: 144-159.

290

291 Koval S, Krahenbuhl G, Warren K and O'Brien G. Optical Microscopy as a New Approach for
292 Characterising Dust Particulates in Urban Environment. *J Environ Manage* 2018; 223: 196-
293 202. doi: 10.1016/j.jenvman.2018.06.038.

294

295 Lebre F, Sridharan R, Sawkins MJ, Kelly DJ, O'Brien FJ and Lavelle EC . The shape and size of
296 hydroxyapatite particles dictate inflammatory responses following implantation. *Sci Rep*.
297 2017; 7: 2922.

298

299 Li W, Shao L, Zhang D, Ro C-U, Hu M, Bi X, Geng H, Matsuki A, Niu H, Chen J. A review of
300 single aerosol particle studies in the atmosphere of East Asia: morphology, mixing state,

301 source, and heterogeneous reactions. Journal of Cleaner Production 2016; 112: 1330-1349.

302 doi.org/10.1016/j.jclepro.2015.04.050.

303

304 Liati A , Spiteri A Eggenschwiler PD and Vogel-Schauble N. Microscopic investigation of

305 soot and ash particulate matter derived from biofuel and diesel: implications for the

306 reactivity of soot. Journal of Nanoparticle Research. 2012; 14: 1224. doi: 10.1007/s11051-

307 012-1224-7

308

309 Liati A, Schreiber D, Eggenschwiler PD, and Dasilva YAR. Metal Particle Emissions in the

310 Exhaust Stream of Diesel Engines: An Electron Microscope Study. Environmental Science &

311 Technology. 2013; 47: 14495-14501. DOI: 10.1021/es403121y

312

313 [Lloyd AC and Cackette TA. Diesel engines: environmental impact and control. J Air Waste](#)

314 [Manag Assoc](#) 2001; 51:809-847.

315

316 Maher BA, Ahmed IA, Karloukovski V, MacLaren DA, Foulds PG, Allsop D, et al. Magnetite

317 pollution nanoparticles in the human brain. Proc Natl Acad Sci U S A. 2016;113(39):10797-

318 801.

319

320 Mäkelä K, Ollila H, Sutinen E, Vuorinen V, Peltola E, Kaarteenaho R, Myllärniemi M. Inorganic

321 particulate matter in the lung tissue of idiopathic pulmonary fibrosis patients reflects

322 population density and fine particle levels. Annals of Diagnostic Pathology 2019; 40: 136-

323 142. doi:10.1016/j.anndiagpath.2019.04.011

324

325 Mills OP, and Rose WI. Shape and surface area measurements using scanning electron
326 microscope stereo-pair images of volcanic ash particles. *Geosphere* 2010; 6: 805–811.
327 doi.org/10.1130/GES00558.1

328

329 Oudin, A., Carlsen, H.K., Forsberg, B., Johansson, C. Volcanic ash and daily mortality
330 in Sweden after the Icelandic volcano eruption of May 2011. *Int. J. Environ. Res. Public*
331 *Health*. 2013; 10, 6909–6919.

332

333 Proussevitch AA, Mulukutla GK and Sahagian DL. A new 3D method of measuring bubble
334 size distributions from vesicle fragments preserved on surfaces of volcanic ash particles.
335 *Geosphere*. 2011; 7: 62–69. doi: 10.1130/GES00559.1

336

337 Ren Y, Yao X, Liu Y, Liu S, Li X, Huang Q, Liu F, Li N, Lu Y, Yuan Z, Li S and Xiang H. Outdoor air
338 pollution pregnancy exposures are associated with behavioral problems in China's
339 preschoolers. *Environ Sci Pollut Res Int*. 2019; 26: 2397-2408.

340

341 Rocha LDS, Corrêa SM. Determination of size-segregated elements in diesel-biodiesel blend
342 exhaust emissions. *Environ Sci Pollut Res*. 2018; 25, 18121–18129. [doi.org/10.1007/s11356-](https://doi.org/10.1007/s11356-018-1980-8)
343 [018-1980-8](https://doi.org/10.1007/s11356-018-1980-8).

344

345 Selley L, Schuster L, Marbach H, Forsthuber T, Forbes B, Gant TW, et al. Brake dust exposure
346 exacerbates inflammation and transiently compromises phagocytosis in macrophages.
347 *Metallomics*. 2020; 12:371-386. doi: 10.1039/c9mt00253g.

348

349 Thurston GD, Balmes JR, Garcia E, et al. Outdoor Air Pollution and New-Onset Airway
350 Disease. An Official American Thoracic Society Workshop Report. *Ann Am Thorac Soc.* 2020;
351 17: 387-398. doi:10.1513/AnnalsATS.202001-046ST
352
353 Tian Y, Liu H, Wu Y, Si Y, Song J, Cao Y, Li M, Wu Y, Wang X, Chen L, Wei C, Gao P, Hu Y.
354 Association Between Ambient Fine Particulate Pollution and Hospital Admissions for Cause
355 Specific Cardiovascular Disease: Time Series Study in 184 Major Chinese Cities. *BMJ* 2019;
356 367:l6572. doi: 10.1136/bmj.l6572.
357
358 Tian ZX, Dietze V, Sommer F, Baum A, Kaminski U, Sauer J, Maschowski C, Stille P, Cen K,
359 Giere R. Coarse-Particle Passive-Sampler Measurements and Single-Particle Analysis by
360 Transmitted Light Microscopy at Highly Frequented Motorways. *Aerosol and Air Quality*
361 *Research.* 2017; 17: 1939–1953.
362
363 Wei Y, Wang Y, Di Q, Choirat C, Wang Y, Koutrakis P, Zanobetti A, Dominici F, Schwartz JD.
364 Short Term Exposure to Fine Particulate Matter and Hospital Admission Risks and Costs in
365 the Medicare Population: Time Stratified, Case Crossover Study. *BMJ.* 2019; 367: l6258. doi:
366 10.1136/bmj.l6258.
367
368 Wertheim D, Gillmore G, Gill I, Petford N. High resolution 3D confocal microscope imaging of
369 volcanic ash particles. *Sci Total Environ.* 2017;590-591:838-42.
370
371 World Health Organisation. Burden of disease from the joint effects of household and
372 ambient Air pollution for 2016. v2 May 2018.

373 https://www.who.int/airpollution/data/AP_joint_effect_BoD_results_May2018.pdf

374 (Accessed 14 May 2020).

375

376 Wu T, Ma Y, Wu X, Bai M, Peng Y, Cai W, Wang Y, Zhao J and Zhang Z. Association between
377 particulate matter air pollution and cardiovascular disease mortality in Lanzhou, China.

378 Environ Sci Pollut Res Int. 2019; 26: 15262-15272.

379

380 Xu N, Lv X, Yu C, Guo Y, Zhang K and Wang Q. The Association Between Short-Term Exposure
381 to Extremely High Level of Ambient Fine Particulate Matter and Blood Pressure: A Panel

382 Study in Beijing, China. Environ Sci Pollut Res Int. 2020 May 15. doi: 10.1007/s11356-020-

383 09126-z

384

385 [Yang, H., X. Li, Y. Wang, M. Mu and G. Kou. Experimental investigation into the oxidation
386 reactivity and nanostructure of particulate matter from diesel engine fuelled with](#)

387 [diesel/polyoxymethylene dimethyl ethers blends. Sci Rep. 2016 Nov 23;6:37611. doi:](#)

388 [10.1038/srep37611.](#)

389

390 Zeb B, Alam K, Sorooshian A, Blaschke T, Ahmad I, Shahid I. On the Morphology and
391 Composition of Particulate Matter in an Urban Environment. Aerosol Air Qual Res.

392 2018;18(6):1431-47.

393

394 [Zhou Q, Wang L, Cao Z, Zhou X, Yang F, Fu P, Wang Z, Hu J, Ding L and Jiang W. Dispersion of
395 atmospheric fine particulate matters in simulated lung fluid and their effects on model cell](#)

396 [membranes. Sci Total Environ. 2016; 542\(Pt A\):36-43. doi: 10.1016/j.scitotenv.2015.10.083.](#)

397

398 **Ethics approval and consent to participate**

399 Not applicable.

400

401 **Consent for publication**

402 Not applicable.

403

404 **Authors Contributions**

405 All authors contributed to devising the study as well as design. LM, GF and IG prepared
406 slides used in this study. LM, GF, GG and DW collected microscope image data used in this
407 study. All authors read and approved the final version of the manuscript.

408

409 **Funding**

410 This work was part funded by Barts Charity, UK (ref: MGU0312) and The Medical College of
411 Saint Bartholomew's Hospital Trust (ref: 17/LO/1752).

412

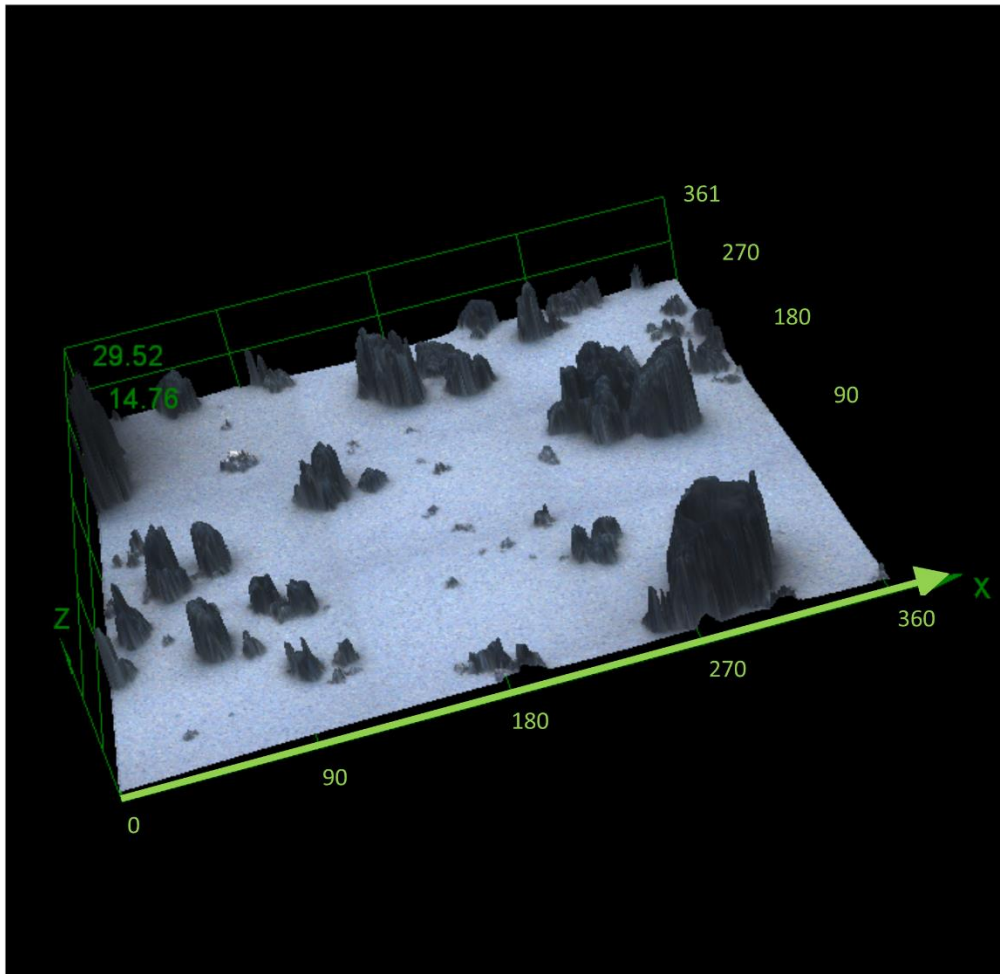
413 **Competing Interests**

414 LM, GF, IG, GG and DW have no competing interests. Professor Grigg received personal fees
415 from AstraZeneca, GSK, Novartis and Vifor Pharma, outside the submitted work. Also
416 Professor Grigg was commissioned by Hodge Jones & Allen Solicitors to provide a medical
417 report to an inquest on air pollution (2020-2021).

418

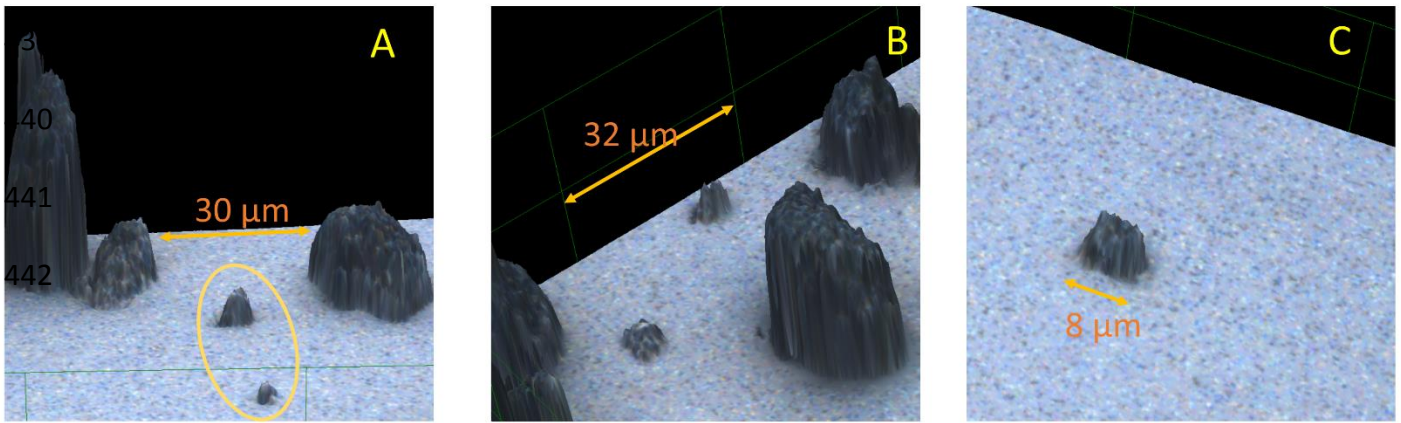
419 **Availability of data and materials**

420 The datasets used and/or analysed during the current study are available from the
421 corresponding author on reasonable request.

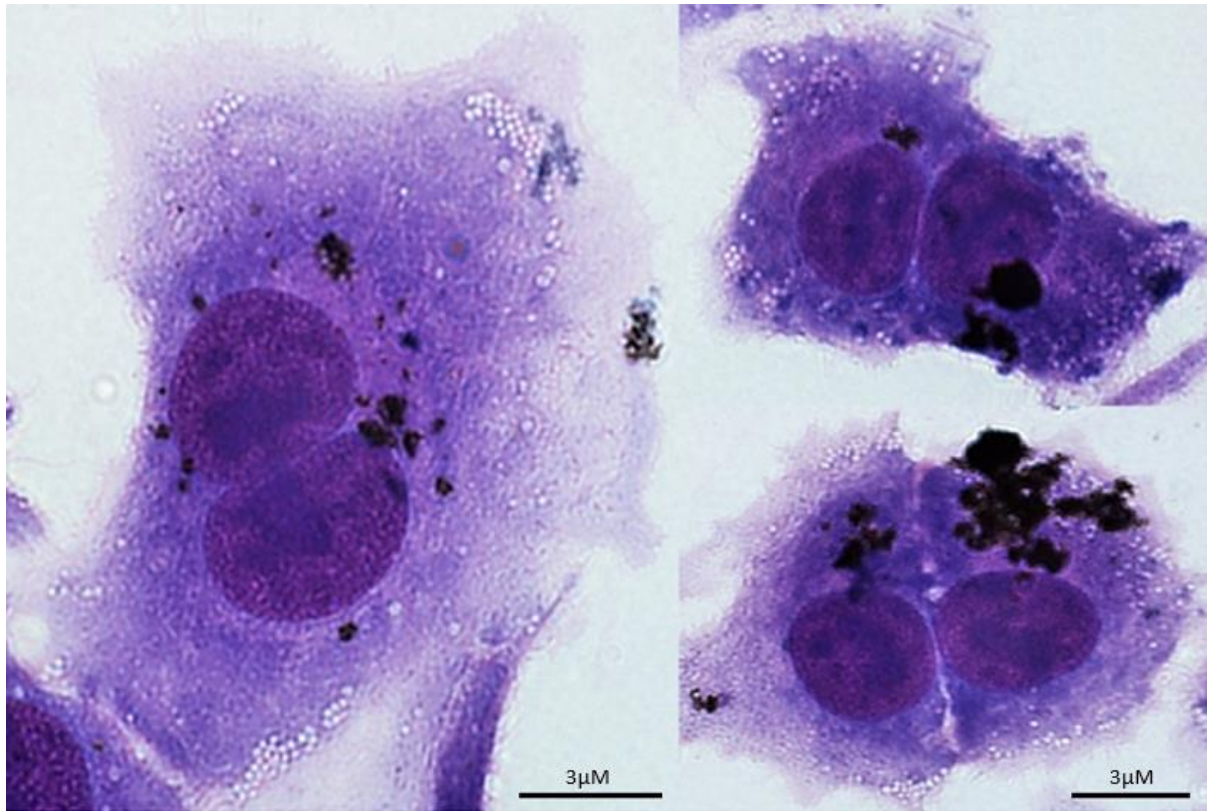


436 **Figure 1:** View of 9 images stitched together to form a region with dimensions 360 x 360 x
437 30 μm ; each of the 9 images was acquired using a x100 objective lens.

438



443 **Figure 2: A)** shows a close-up of two PM₁₀ particles in orange oval (4.8 by 4.4, max height
 444 2.8 and 2.8 by 2.4, max height 1.3 µm) surrounded by three large particle aggregates with
 445 max heights of 19.9, 4.4 and 7.6 µm (left to right); **B)** close-up of one of the constituent
 446 stitched images in panel (A) with two PM₁₀ particles with major and minor axes dimensions
 447 of 5.6 by 4.5 (max height 3.1) and 5.8 by 4.9 (max height 2.2) µm; one of the particles in
 448 particular appears to have a sharp protruding surface; the orange scale bar indicates linear
 449 distance of 32 µm; **C)** image obtained with a x100 objective lens is a zoomed in close-up
 450 showing another sharp appearing particle with major and minor axes dimensions of 7.7 by
 451 7.0 (max height 3.7) µm. For clarity all images have a z axis factor of 2 which magnifies the
 452 relative z axis component visualisation.



453

454 **Figure 3:** Image of six A549 lung epithelial cells exposed to 10 µg/ml DPM. DPM is observed
455 to be adherent to cells.

456

457

458

459

460

